Stanford Exploration Project, Report 120, May 3, 2005, pages 63–76

Imaging steeply dipping reflectors in TI media by wavefield extrapolation

Guojian Shan and Biondo Biondi[1]

ABSTRACT

We develop an anisotropic plane-wave migration method based on wavefield extrapolation. In this new scheme, we decompose both source and receiver wavefields into plane waves by delaying shots. For each plane wave, we design a tilted coordinate system whose tilting angle depends on the propagation direction of the plane wave. The wavefield extrapolation is done by an implicit isotropic operator plus an explicit anisotropic correction operator. We apply this method on a synthetic dataset. The results show that our scheme can accurately handle overturned waves and image steeply dipping reflectors in transversely isotropic media with a vertical axis of symmetry (VTI).

INTRODUCTION

VTI media is one of the simplest and most practically important types of anisotropic media. Steeply dipping structures, such as faults and salt flanks, are important for the interpretation of seismic data. The waves relating to steeply dipping reflectors usually propagate in a direction far from vertical. If we do not account for the anisotropy in the migration, steeply dipping reflectors will be imaged with large positional errors or will vanish from the image. To image steeply dipping reflectors in anisotropic media, we need an anisotropic wavefield-extrapolation operator that can handle waves propagating in a direction far from the vertical direction.

Many methods have been proposed to extrapolate wavefields and image reflectors in VTI or tilted TI media (Ristow and Ruhl, 1997; Rousseau, 1997; Ferguson and Margrave, 1998; Uzcategui, 1995; Zhang et al., 2001a,b). Baumstein and Anderson (2003) extrapolate wavefields in VTI media with a reference anisotropic phase-shift operator plus an explicit correction filter. Shan and Biondi (2004b) extrapolate wavefields in tilted TI media with an isotropic operator followed by an explicit anisotropic correction filter.

The waves related to steeply dipping reflectors usually propagate far from the vertical direction. Kirchhoff methods can propagate these waves correctly, but they are less reliable for imaging complex structure because of the high-frequency approximation. Reverse-time migration (Whitmore, 1983; Baysal et al., 1983; Biondi and Shan, 2002), which is based on the two-way wave equation, can propagate these waves accurately; however anisotropic

[1]**email:** shan@sep.stanford.edu, biondo@sep.stanford.edu

reverse-time migration is still prohibitively expensive. Algorithms such as beam migration (Brandsberg-Dahl and Etgen, 2003; Hill, 2001; Gray et al., 2002; Albertin et al., 2001) and coordinate-transformation-based migration (Higginbotham et al., 1985; Etgen, 2002; Sava and Fomel, 2004; Shan and Biondi, 2004a), extrapolate wavefields in a direction close to the propagation direction, and can handle these waves at a wide angle.

In this paper, we apply plane-wave migration in tilted coordinates for VTI media. VTI media in Cartesian coordinates become to tilted TI media in tilted coordinates. We extrapolate the wavefields with an isotropic operator followed by an explicit anisotropic correction. We first discuss VTI media in tilted coordinates, then review plane-wave migration in tilted coordinates, and finally show the migration results for a synthetic dataset.

VTI MEDIA IN TILTED COORDINATES

A VTI medium is a medium that is transversely isotropic and has a vertical axis of symmetry. The phase-velocity $V(\theta)$ of P-waves in VTI media can be expressed in Thomsen notation as follows (Tsvankin, 1996):

$$\frac{V^2(\theta)}{V_{P0}^2} = 1+\varepsilon\sin^2(\theta)-\frac{f}{2}\pm\frac{f}{2}\sqrt{\left(1+\frac{2\varepsilon\sin^2(\theta)}{f}\right)^2-\frac{2(\varepsilon-\delta)\sin^2(2\theta)}{f}}, \tag{1}$$

where θ is the phase angle of the propagating wave, and $f = 1-(V_{S0}/V_{P0})^2$. V_{P0} and V_{S0} are the P- and SV-wave velocities in the vertical direction, respectively, and ε and δ are anisotropy parameters defined by Thomsen (1986):

$$\varepsilon = \frac{C_{11}-C_{33}}{2C_{33}}, \delta = \frac{(C_{11}+C_{44})^2-(C_{33}-C_{44})^2}{2C_{33}(C_{33}-C_{44})},$$

where C_{ij} are elastic moduli. In equation (1), $V(\theta)$ is the P-wave phase-velocity when the sign in front of the square root is positive, and the SV-wave phase velocity for a negative sign.

For plane-wave propagation, the phase angle θ is related to the wavenumbers k_x and k_z by the following relations:

$$\sin\theta = \frac{V(\theta)k_x}{\omega}, \qquad \cos\theta = \frac{V(\theta)k_z}{\omega}, \tag{2}$$

where ω is the temporal frequency. From Cartesian coordinates to tilted coordinates, we do a transformation as follows:

$$\begin{pmatrix} x' \\ z' \end{pmatrix} = \begin{pmatrix} \cos\varphi & \sin\varphi \\ -\sin\varphi & \cos\varphi \end{pmatrix} \begin{pmatrix} x \\ z \end{pmatrix}. \tag{3}$$

where φ is the rotation angle.

Figure 1 illustrates this change of symmetry axis during the coordinate transformation. The layered structure has a symmetry axis in the vertical direction in Cartesian coordinates

(x,z) in the left panel. When we rotate the coordinates from (x,z) to (x',z'), the symmetry axis in the new coordinates (x',z') deviates from the z' direction.

In tilted coordinates (x',z'), we have the following relation between wavenumber $k_{x'},k_{z'}$ and phase angle θ':

$$\sin\theta' = \frac{V(\theta')k_{x'}}{\omega}, \qquad \cos\theta' = \frac{V(\theta')k_{z'}}{\omega}. \tag{4}$$

The symmetry axis is not vertical in tilted coordinates, so the angle between the direction of wave propagation and the symmetry axis is not the phase angle θ', but $\theta'-\varphi$, where φ is the tilting angle of the tilted coordinates.. Therefore, VTI media in Cartesian coordinates become tilted TI media. The P-wave phase velocity in tilted coordinates can be expressed as

$$\frac{V^2(\theta',\varphi)}{V_{P0}^2} = 1+\varepsilon\sin^2(\theta'-\varphi) - \frac{f}{2} \pm \frac{f}{2}\sqrt{\left(1+\frac{2\varepsilon\sin^2(\theta'-\varphi)}{f}\right)^2 - \frac{2(\varepsilon-\delta)\sin^2(2(\theta'-\varphi))}{f}}. \tag{5}$$

Thus for a VTI medium in tilted coordinates we need a wave-extrapolation operator that can

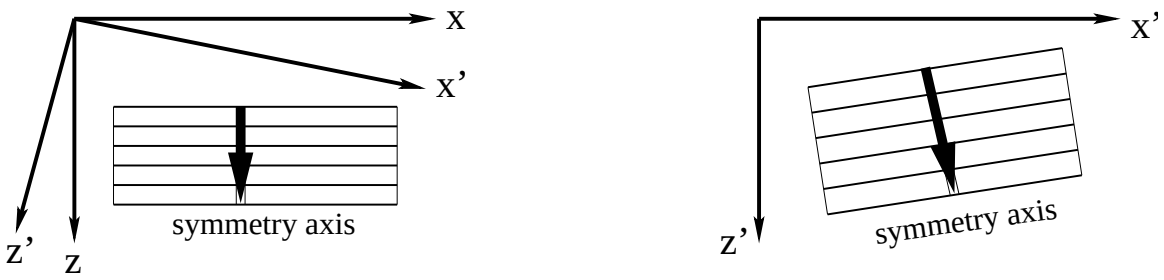

Figure 1: VTI media in tilted coordinates. Left panel is a layer structure in Cartesian coordinates. Right panel is the layer structure in tilted coordinates. guojian1-vtitilt [NR]

downward extrapolate the wavefield in tilted TI media. From equations (4) and (5), we can solve $k_{z'}$ as a function of $\varphi,\varepsilon,\delta$, and ω/V_{P0}. The wavefield can be extrapolated in two steps. First, the wavefield is extrapolated by an isotropic operator as follows:

$$\bar{P}(z+\Delta z) = P(z)e^{ik_z^{iso}\Delta z}, \tag{6}$$

where $k_z^{iso} = \sqrt{(\omega/V_{P0})^2-(k_x')^2}$ is the isotropic vertical spatial wavenumber. This isotropic operator can be implemented by the split-step method (Stoffa et al., 1990), the general screen propagator (Huang and Wu, 1996), or Fourier finite difference (FFD) (Ristow and Ruhl, 1994). Next, the wavefield is corrected by an explicit correction operator. This correction operator is designed in the Fourier domain, and is implemented in the space domain. The correction operator in the Fourier domain is a phase-shift operator:

$$P(z+\Delta z) = \bar{P}(z+\Delta z)e^{i(k_z'-k_z^{iso})\Delta z}. \tag{7}$$

In the space domain, this correction operator is a convolution filter. The coefficients of the convolution filter depend on $\varphi,\varepsilon,\delta$, and ω/V_{P0}, and they can be estimated by the weighted least-squares method (Shan and Biondi, 2004b).

ANISOTROPIC PLANE-WAVE MIGRATION IN TILTED COORDINATES

In plane-wave migration (Rietveld, 1995; Duquet et al., 2001; Liu et al., 2002; Zhang et al., 2003) source wavefields are decomposed into plane waves, and the receiver wavefields are re-arranged corresponding to their respective plane-wave source. Shan and Biondi (2004a) apply plane-wave migration in tilted coordinates for an isotropic medium. For each plane wave, proper tilted coordinates are designed, whose tilting angle is selected according to the direction in which the plane wave propagates. Source and receiver wavefields are downward continued in these tilted coordinates. Images and dip-dependent angle-domain common-image gathers (CIGs) are generated by cross-correlation.

Anisotropic plane-wave migration is the same as isotropic plane-wave migration, except that an anisotropic correction operator is applied after the isotropic wavefield extrapolation at each depth step. Since the correction operator is explicit, we build a table of convolution coefficients before we run the wavefield extrapolation. If the medium at a point in space is isotropic ($\varepsilon = \delta = 0$), only the isotropic extrapolation will occur. Otherwise, the anisotropic correction operator will be applied to the wavefield. For anisotropic correction, we search for the filter coefficients corresponding to the tilting angle φ, anisotropy parameters ε and δ and the value of ω / V_{P0} in the table and convolve the wavefield at that spatial position with these coefficients. As in the isotropic case, images and dip-dependent angle-domain CIGs can be created by cross-correlating the source and receiver wavefields.

NUMERICAL EXAMPLE

We test our method on a synthetic dataset and compare the results of isotropic and anisotropic migration. Figure 2 shows the model of the synthetic data we use to test our method. Figure 2(a) is the density model, Figure 2(b) is the vertical P-wave velocity model, and Figure 2(c) is the map of the anisotropy parameter ε. The anisotropy parameter δ is 0 for this dataset. The salt flank is very steep, and its top part over hangs. In the sediments, the vertical P-velocity increases gradually with the depth. One sediment layer (between 2000 m and 3000 m) is strongly anisotropic. Our aim is to image the flank of the salt dome and the sediment reflector below the anisotropic layer and near the salt dome accurately. Figure 3 shows a near-offset section of the synthetic data. Notice the strong energy reflected from the salt flank in the near offset data.

Figure 4 shows the results of the isotropic migration for this dataset. Figure 4(a) is the result of the isotropic plane-wave migration in Cartesian coordinates, and Figure 4(b) is the result of the isotropic plane-wave migration in tilted coordinates. In Figure 4(a), the salt flank is totally lost. This is because waves related to the salt flank are overturned, and the one-way wave-equation downward continuation method can not extrapolate them correctly. In Figure 4(b), although a weak steeply dipping reflector can be seen, it is not at the correct position, because the anisotropy in the sediment layer was neglected.

Figure 5 shows the results of the anisotropic migration for this dataset. Figure 5(a) is the anisotropic plane-wave migration in Cartesian coordinates, and Figure 5(b) is the anisotropic

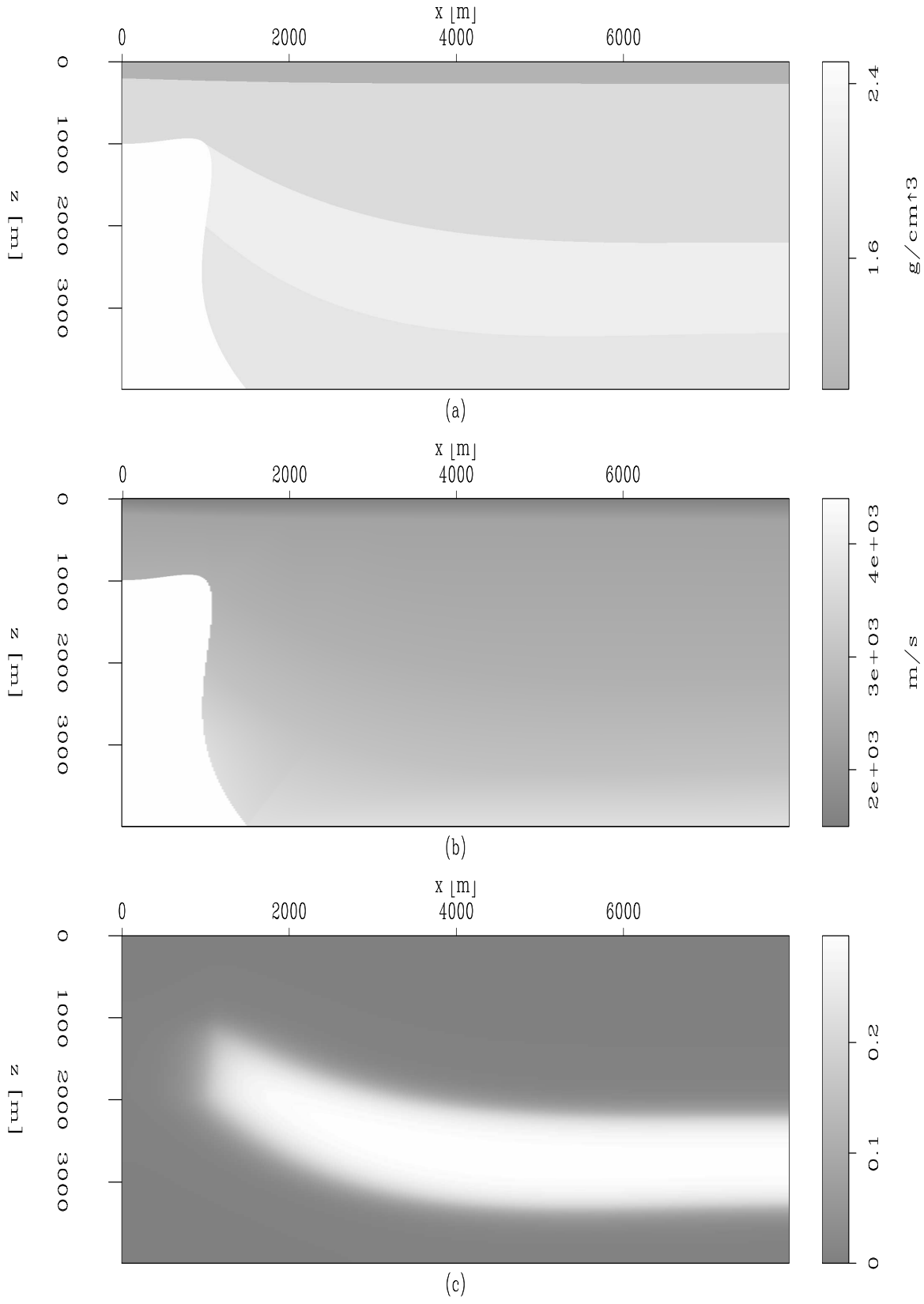

Figure 2: Model of the synthetic dataset. (a) Density model; (b) Velocity model; (c) Anisotropy parameter ε. guojian1-model [ER]

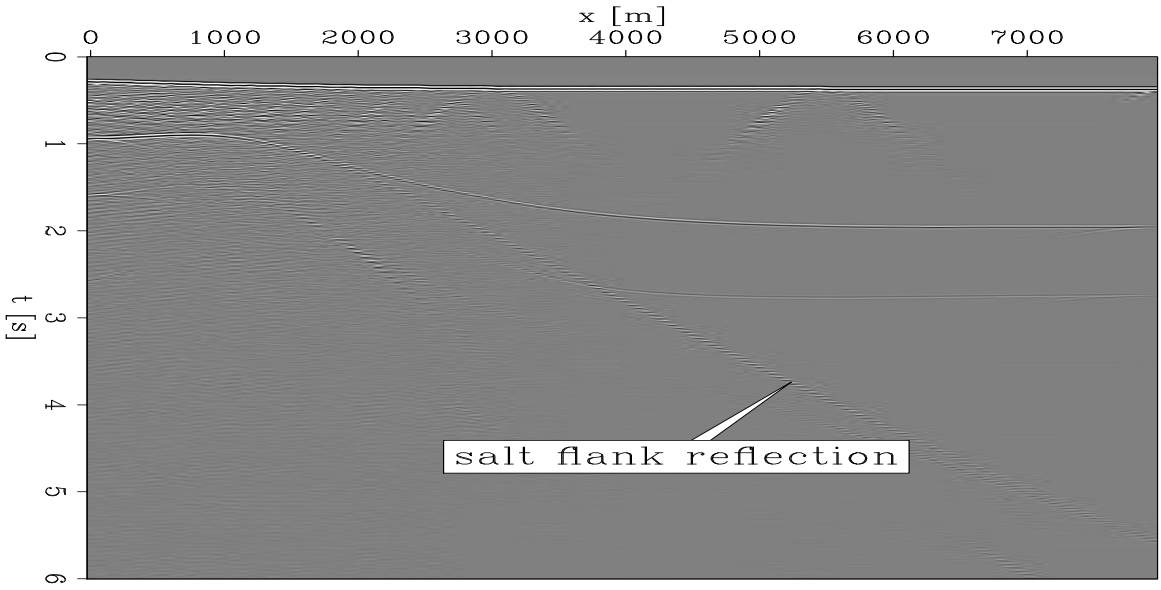

Figure 3: A near-offset section of the synthetic data. guojian1-nearoffset [ER]

plane-wave migration in tilted coordinates. In Figure 5(a), the top part of the salt flank is lost due to overturned waves, but the bottom part of the salt flank is correctly imaged, but is not focused by the isotropic migration (Figures 4(a) and 4 (b)). In Figure 5(b), the image is greatly improved compared to the previous three images. Both the top and bottom parts of the salt flank are well imaged. In Figure 5(b), the reflector below the anisotropic layer is stronger and more continuous near the salt flank compared to that in the isotropic migration result. To check if the reflectors are imaged at the correct positions, we overlay the images with the density model in Figure 6. Figure 6(a) is the isotropic migration result overlaid with the density model. Figure 6(b) is the anisotropic migration result overlaid with the density model. The salt flank matches the density model very well in the image obtained by the anisotropic migration, while it deviates from the model in the isotropic one. The flat part of the reflector below the anisotropic layer is not affected much by the anisotropy. Both the isotropic and anisotropic migration image it at the correction position.

Figure 7 shows the horizontal angle-domain CIGs at the horizontal location $x = 4000$m. Figure 7(a) is obtained by the isotropic migration, and Figure 7(b) is obtained by the anisotropic migration. Figure 8 shows the vertical angle-domain CIGs at the vertical location $z = 1500$m. Figure 8(a) is obtained by the isotropic migration, and Figure 8(b) is obtained by the anisotropic migration. Although we use the true, vertical P-wave velocity in the isotropic migration, we find a small curvature in the horizontal angle gathers at the reflector below the anisotropic layer (at $z = 3300$ m in Figure 7), and a big curvature in the vertical angle gathers at the salt flank (x between 1000 m and 1500 m in Figure 8). In the anisotropic migration, the angle gathers are flat at these locations. The big curvature of the angle gathers at the steeply dipping reflectors can be used as a tool to estimate the error in the anisotropy parameters used in the migrations.

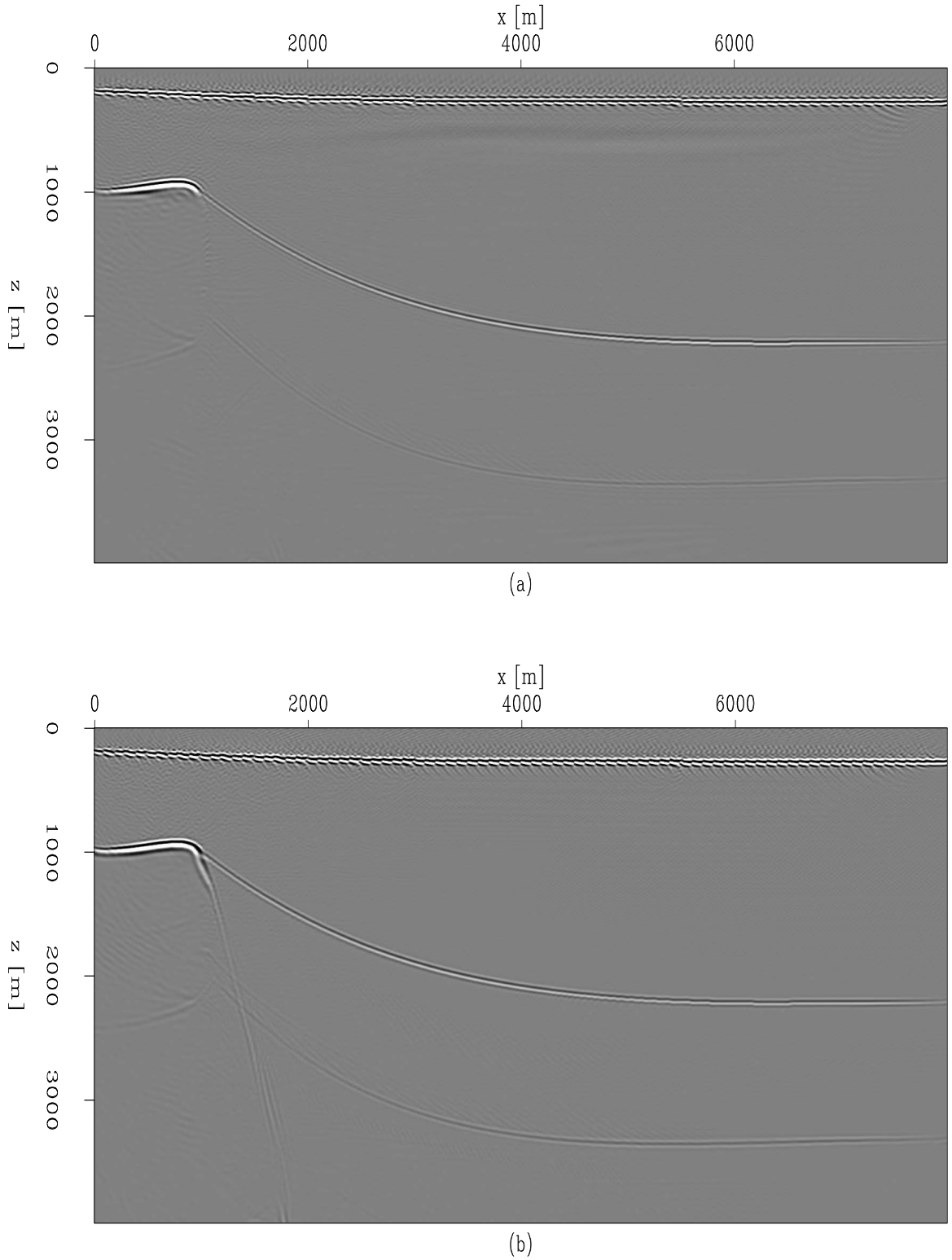

Figure 4: Isotropic plane-wave migration results: (a) in Cartesian coordinates; (b) in tilted coordinates. guojian1-iso [CR]

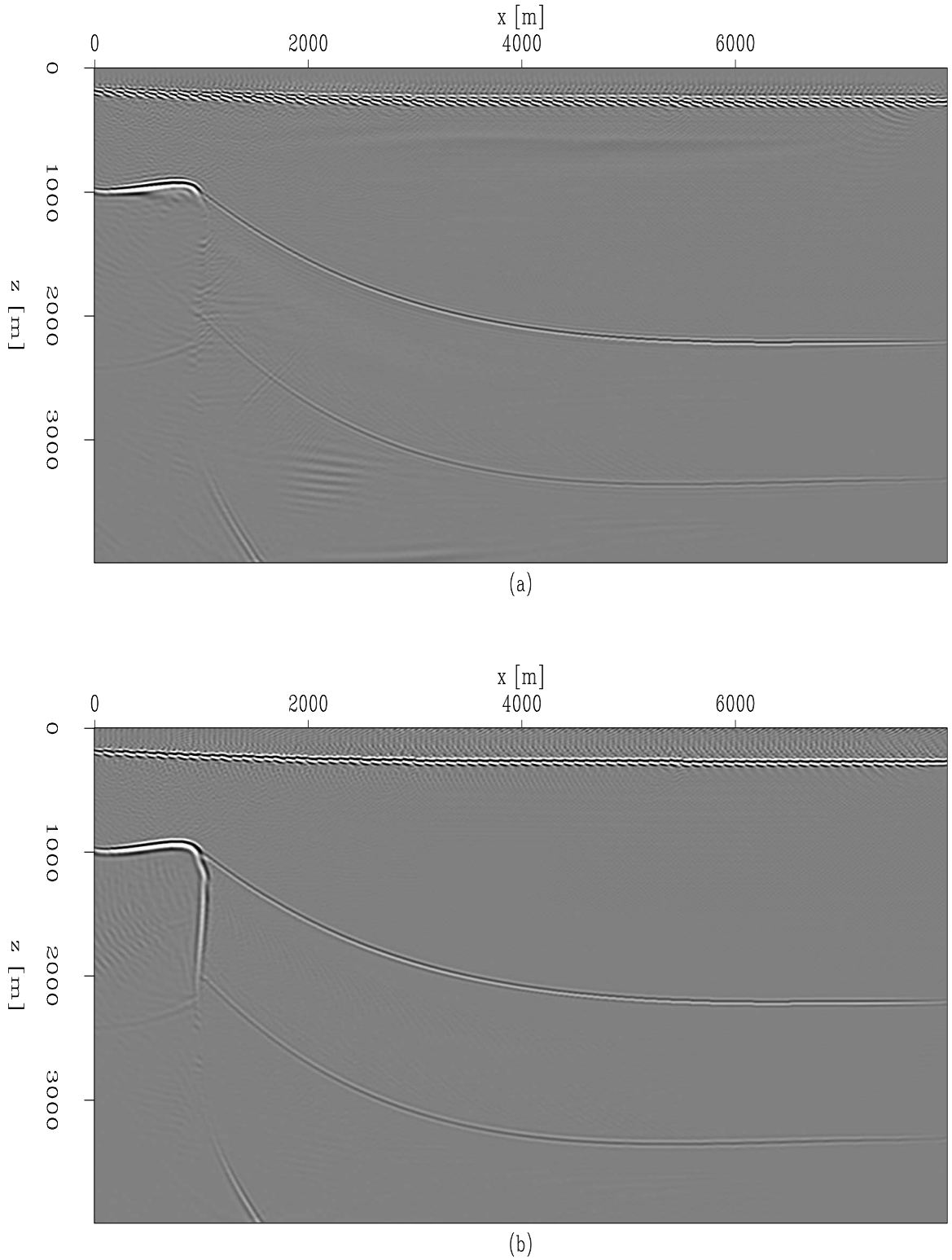

Figure 5: Anisotropic plane-wave migration results: (a) in Cartesian coordinates; (b) in tilted coordinates. guojian1-ani [CR]

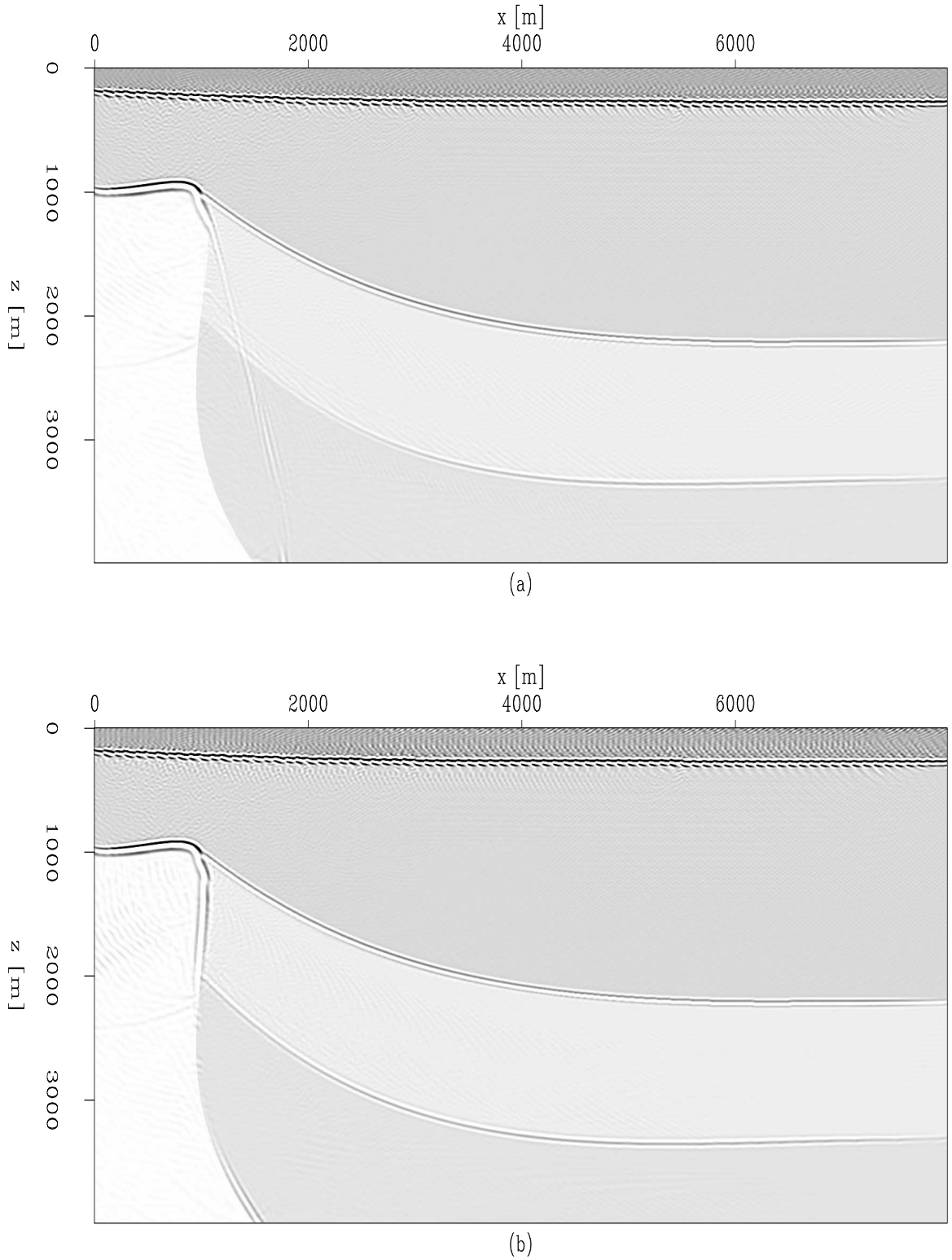

Figure 6: Migration results overlaid with density model: (a) isotropic migration; (b) anisotropic migration. guojian1-isoanidn [CR]

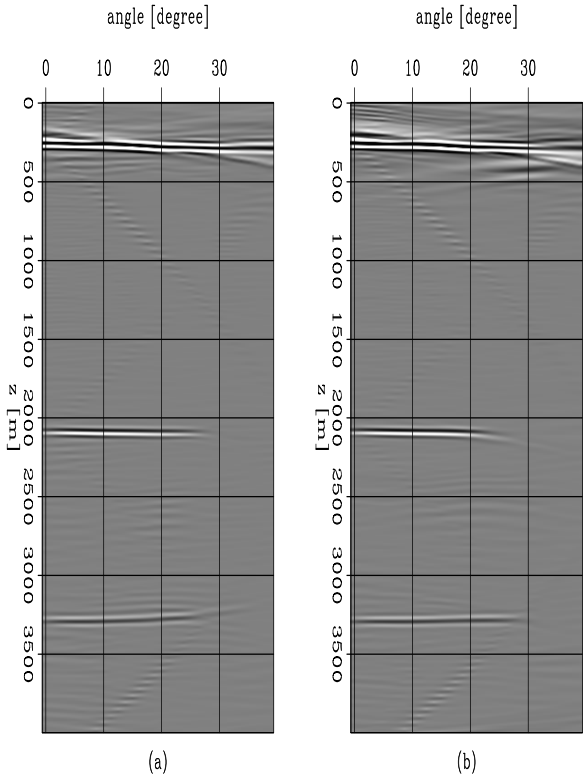

Figure 7: Horizontal angle-domain CIGs at $x = 4000$m: (a) isotropic migration; (b) anisotropic migration. guojian1-ang4000 [CR]

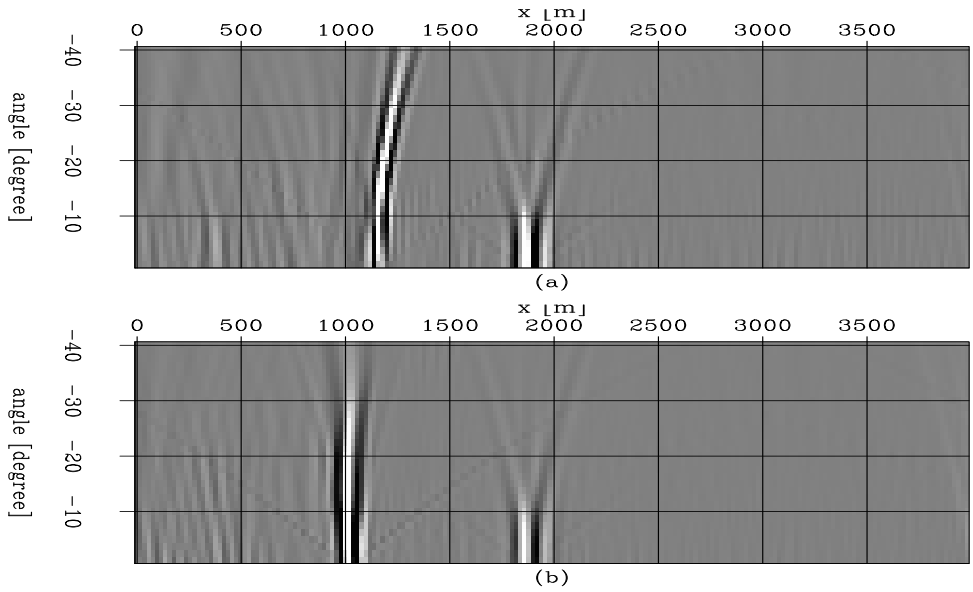

Figure 8: Vertical angle-domain CIGs at $z = 1500$m: (a) isotropic migration; (b) anisotropic migration. guojian1-ang1500 [CR]

CONCLUSION

We image steeply dipping reflectors in VTI media by anisotropic plane-wave migration in tilted coordinates. We decompose source and receiver wavefields into plane waves and extrapolate the wavefields with an implicit isotropic operator followed by an explicit anisotropic correction in tilted coordinates. We apply our method to a synthetic dataset. The results show that our method can handle overturned waves and accurately image steeply dipping reflectors in VTI media. We generate angle-domain CIGs by cross-correlation.

ACKNOWLEDGMENTS

We would like to thank ExxonMobil for making the synthetic data available.

REFERENCES

Albertin, U., Yingst, D., and Jaramillo, H., 2001, Comparing common-offset Maslov, Gaussian beam, and coherent state migrations *in* 71st Ann. Internat. Mtg. Soc. of Expl. Geophys., 913–916.

Baumstein, A., and Anderson, J., 2003, Wavefield extrapolation in laterally varying VTI media *in* 73rd Ann. Internat. Mtg. Soc. of Expl. Geophys., 945–948.

Baysal, E., Kosloff, D. D., and Sherwood, J. W. C., 1983, Reverse time migration: Geophysics, **48**, 1514–1524.

Biondi, B., and Shan, G., 2002, Prestack imaging of overturned reflections by reverse time migration *in* 72nd Ann. Internat. Mtg. Soc. of Expl. Geophys., 1284–1287.

Brandsberg-Dahl, S., and Etgen, J., 2003, Beam-wave imaging *in* Expanded Abstracts. Soc. of Expl. Geophys., 977–980.

Duquet, B., Lailly, P., and Ehinger, A., 2001, 3-D plane wave migration of streamer data *in* 71st Ann. Internat. Mtg. Soc. of Expl. Geophys., 1033–1036.

Etgen, J., 2002, Waves, beams and dimensions: an illuminating if incoherent view of the future of migration: 72nd Ann. Internat. Mtg, Soc. of Expl. Geophys., invited presentation.

Ferguson, R. J., and Margrave, G. F., 1998, Depth migration in TI media by nonstationary phase shift *in* 68th Ann. Internat. Mtg. Soc. of Expl. Geophys., 1831–1834.

Gray, S., Notfors, C., and Bleistein, N., 2002, Imaging using multi-arrivals: Gaussian beams or multi-arrival Kirchhoff? *in* 72nd Ann. Internat. Mtg. Soc. of Expl. Geophys., 1117–1120.

Higginbotham, J. H., Shin, Y., and Sukup, D. V., 1985, Directional depth migration (short note): Geophysics, **50**, 1784–1796.

Hill, N. R., 2001, Prestack Gaussian-beam depth migration: Geophysics, **66**, 1240–1250.

Huang, L. Y., and Wu, R. S., 1996, Prestack depth migration with acoustic screen propagators *in* 66th Ann. Internat. Mtg. Soc. of Expl. Geophys., 415–418.

Liu, F., Stolt, R., Hanson, D., and Day, R., 2002, Plane wave source composition: An accurate phase encoding scheme for prestack migration *in* 72nd Ann. Internat. Mtg. Soc. of Expl. Geophys., 1156–1159.

Rietveld, W. E. A., 1995, Controlled illumination of prestack seismic migration *in* Ph.D. thesis. Delft University of Technology.

Ristow, D., and Ruhl, T., 1994, Fourier finite-difference migration: Geophysics, **59**, 1882–1893.

—, 1997, Migration in transversely isotropic media using implicit operators *in* 67th Ann. Internat. Mtg. Soc. of Expl. Geophys., 1699–1702.

Rousseau, J. H. L., 1997, Depth migration in heterogeneous, transversely isotropic media with the phase-shift-plus-interpolation method *in* 67th Ann. Internat. Mtg. Soc. of Expl. Geophys., 1703–1706.

Sava, P., and Fomel, S., 2004, Wavefield extrapolation in Riemannian coordinates *in* Expanded Abstracts. Soc. of Expl. Geophys.

Shan, G., and Biondi, B., 2004a, Imaging overturned waves by plane-wave migration in tilted coordinates: 74th Ann. Internat. Mtg., Soc. of Expl. Geophys., Expanded Abstracts, 969–972.

—, 2004b, Wavefield extrapolation in laterally-varying tilted TI media: SEP– **117**, 1–10.

Stoffa, P. L., Fokkema, J. T., de Luna Freire, R. M., and Kessinger, W. P., 1990, Split-step Fourier migration: Geophysics, **55**, 410–421.

Thomsen, L., 1986, Weak elastic anisotropy: Geophysics, **51**, 1954–1966.

Tsvankin, I., 1996, P-wave signatures and notation for transversely isotropic media: An overview: Geophysics, **61**, 467–483.

Uzcategui, O., 1995, 2-D depth migration in transversely isotropic media using explicit operators: Geophysics, **60**, 1819–1829.

Whitmore, N. D., 1983, Iterative depth migration by backward time propagation *in* 53rd Ann. Internat. Mtg. Soc. of Expl. Geophys., Session:S10.1.

Zhang, J., Verschuur, D. J., and Wapenaar, C. P. A., 2001a, Depth migration of shot records in heterogeneous, tranversely isotropic media using optimum explicit operators: Geophys. Prosp., **49**, 287–299.

Zhang, J., Wapenaar, C., and Verschuur, D., 2001b, 3-D depth migration in VTI media with explicit extrapolation operators *in* 71st Ann. Internat. Mtg. Soc. of Expl. Geophys., 1085–1088.

Zhang, Y., Sun, J., Notfors, C., and Gray, S., 2003, Delayed-shot 3-D prestack depth migration *in* Expanded Abstracts. Soc. of Expl. Geophys., 1027–1030.